Impregnation of Chitosan onto Activated Carbon for Adsorption Selectivity Towards CO2: Biohydrogen Purification

Article *in* KMUTNB International Journal of Applied Science and Technology · April 2016

DOI: 10.14416/j.ijast.2016.03.003

CITATIONS
10

READS
17

3 authors, including:

Naparat Pairin
King Mongkut's University of Technology North Bangkok
1 PUBLICATION **10** CITATIONS

SEE PROFILE

Chan Phalakornkule
King Mongkut's University of Technology North Bangkok
88 PUBLICATIONS **1,615** CITATIONS

SEE PROFILE

Research Article

Impregnation of Chitosan onto Activated Carbon for Adsorption Selectivity Towards CO_2: Biohydrogen Purification

Jarint Foungchuen, Naparat Pairin and Chantaraporn Phalakornkule*
Department of Chemical Engineering, The Research and Technology Center for Renewable Products and Energy, King Mongkut's University of Technology North Bangkok, Bangkok, Thailand

* Corresponding author. E-mail: cpk@kmutnb.ac.th DOI: 10.14416/j.ijast.2016.03.003
Received: 1 March 2016; Accepted: 28 March 2016; Published online: 21 April 2016

Abstract
In this study, a novel bio-based adsorbent was developed for biohydrogen purification by an adsorption process. Palm shell activated carbons were immersed in the chitosan solutions at the concentrations between 0.1–2 g/L. The results showed that the impregnation of chitosan onto activated carbons at every concentration under the investigation changed the BET surface areas, pore size distribution, CO_2 adsorption capacity and the CO_2/H_2 selectivity. The chitosan impregnated activated carbon that was the most suitable for carbon dioxide/hydrogen separation was the one impregnated in the 0.1 g/L chitosan solution yielding 0.12 g chitosan per 100 gram activated carbon. The modified activated carbon was found to have 11% higher CO_2 adsorption capacity than the native activated carbon even though its BET surface area was reduced by 3% due to the impregnation process. From a lab-scale pressure swing adsorption process using the modified activated carbon as the adsorbent (under an adsorption pressure of 4 bar and the feed flow rate of 2 L/min 50-30-20 mixture of CO_2, H_2 and N_2 for a period of 2 min per cycle), the CO_2 concentration in the effluent was not detected for at least 5 cycles.

Keywords: Modified activated carbon, Chitosan, Impregnation, Biohydrogen, Hydrogen purification

1 Introduction

As our world is facing both energy and environmental management problems, renewable energy has received special attention in recent years. Renewable energy can reduce the dependence on petroleum and other fossil fuels and furthermore it is more environmentally friendly. Hydrogen is an alternative energy that is clean and has the potential to replace fossil fuel. Hydrogen contains high energy value and releases only water when combusted. The heating value is 282 kJ per mole of H_2O generated [1]. A well known method for hydrogen production is a steam reforming process which yields a gas mixture with a typical composition of hydrogen 87%, carbon dioxide 11%, carbon monoxide 0.5–1% and methane 1–2%. An alternative hydrogen production is by a biological process which yields a gas mixture with a typical composition of hydrogen (H_2 50–60% v/v), methane (CH_4 10–20%), carbon dioxide (CO_2 30–40%) and few percentages of water. The separation of carbon dioxide from hydrogen is a necessary step to upgrade biohydrogen. Purified hydrogen can be acquired by a gas separation process such as pressure swing adsorption. There are variety types of adsorbent for the adsorption process. Some of them are available naturally while the others are synthesized such as zeolite, silica gel, activated alumina and activated carbons.

Activated carbon offers an attractive and inexpensive adsorbent for removing several solutes from aqueous solutions as well as from gaseous environment. The activated carbons may differ mainly

Please cite this article as: J. Foungchuen, N. Pairin, and C. Phalakornkule, "Impregnation of chitosan onto activated carbon for adsorption selectivity towards CO_2: biohydrogen purification," *KMUTNB Int J Appl Sci Technol*, vol. 9, no. 3, pp. 197–209, July–Sept. 2016.

in pore size distribution and surface polarity [2]. In the literuature, chemical modification of the adsorbent surface was performed in order to enhance selectivity and chelating ability. The reactive adsorption allows both the separation of target gases from a gas mixture and the capture and storage of the target gases. Surface of the adsorbnet can be modified by various methods, such as ammonia treatment [3], chemical oxidation [4], carbon chemically activated with H_3PO_4 [5] and chemical impregnation [6], [7]. These methods can create the selectivity based on the chemical interactions between polar molecules and the adsorbents. An impregnation process has been successfully used as a method to introduce amines-based molecules onto the surface of AC. Amine-impregnation is a convenient method for increasing CO_2 adsorption especially at elevated temperatures [8]–[11]. The amine-impregnation was found to increase the selectivity of the adsorbent towards CO_2 because amino groups provide specific adsorption sites with stronger intercations than van der Waals forces [9]. In addition, it has been reported that the energy required for regeneration of the adsorbent in the chemical adsorption process is less than the energy required for regeneration of the solvents in the chemical absorption process [12].

In our previous work [13], the activated carbon with modified surface polarity was prepared with an environmentally friendly material, chitosan a biopolymer or poly-[β(1→4)-2-amino-2-deoxy-D-glucopyranose]. Chitosan is mainly produced by alkaline deacetylation of chitin [14]–[16]. The structure of chitin and chitosan is similar to cellulose except that the C-2-hydroxyl group of cellulose is replaced by an acetamido and amino group, respectively. Chitosan is insoluble in most organic solvents but it dissolves in acidic solutions [17]. Chitosan is expected to have high affinity to CO_2 because its amine groups are specific for CO_2 chemisorption via the carbamate-forming reaction [8]–[11].

In this study, modified activated carbon was prepared by impregnating chitosan onto activated carbons. The effect of the amount of chitosan impregnated onto activated carbon (AC) on the surface characteristics of the adsorbent was investigated. The static CO_2 adsorption and the dynamic separation of $CO_2/N_2/H_2$ gas mixture, in which N_2 was used to represent CH_4 in biohydrogen, were investigated on the modified activated carbon. Potential uses of the modified activated carbon for CO_2 capture and storage were discussed.

2 Materials and Methods

2.1 *Activated carbon and chitosan*

Palm shell activated carbon produced by physical activation process with steam as the activating agent was obtained from C. Gigantic Carbon Co., Ltd. (Thailand). The characteristics of the activated carbon are reported in Table 1.

Table 1: Properties of the palm shell activated carbon (the native activated carbon, AC)

Characteristics	Measurement Method	Value
Bulk density	ASTM D2854	0.59 g/cm^3
Particle size distribution	ASTM D2862	91% (PASS 200MESH)
Iodine absorption	ASTM D4607	862.0 mg/g
pH value	ASTM D3838	10.1
Ash content	ASTM D2863	6.1%

Gases CO_2, H_2 and N_2 were of analytical grades (99.995%). The chitosan was provided by Taming Enterprises Co., Ltd. (Thailand) and its characteristics are as follows: degree of deacetylation = 93.8%; molecular weight = 17,010 Da; moisture content = 7%; ash content = 0.95%; protein content = 3.01%; viscosity = 27.40×10^{-3} Pa s. Chitosan solution (2% w/v) was prepared by mixing 2 g of chitosan in 900 mL of 1 M acetic acid. The solution was mixed at 200 rpm for 24 h. One hundred mL of 1 M sodium acetate was added and agitated for 1 h.

2.2 *Chitosan impregnation onto activated carbon*

The activated carbons were washed with deionized water to remove fines and dirt and then oven dried at 378 K for 24 h before the impregnation process was conducted. The AC was sieved to sizes ranging from 3–4 mm and divided in 2 g portions and placed in separate Erlenmeyer flasks and 50 mL of chitosan solutions with initial concentrations of 0.1–2.0 g/L were added. The AC together with the chitosan solution was then agitated in an orbital shaker at 180 rpm at 298 K for 3 days.

The AC was separated from the chitosan solution by filtration. Chitosan concentration was indicated by an absorbance value measured by UV-vis spectrophotometer

(Thermo Scientific, Genesys 10S UV-Vis, USA) at the wavelength of 202 nm. The percentage amount of chitosan impregnated onto the activated carbon was calculated by equation (1).

$$\%wt = \frac{(C_o - C_e)V}{m} \times 100 \quad (1)$$

where $\%wt$ is the equilibrium amount of chitosan impregnated onto activated carbon. C_o and C_e is the initial and equilibrium concentration (g/L) of chitosan in solution. V is the volume (L) of the chitosan solution. m is the weight (g) of activated carbon.

The chitosan impregnated activated carbon (CHI/AC) was oven dried at 378 K for 24 h. The amount of chitosan impregnated on the activated carbon was cross-checked by a calculation of the difference between the weight of chitosan before and after the impregnation process. In addition, before each adsorption test, all adsorbent was heated at 378 K for 24 h.

2.3 *Characterization*

All the adsorbent samples were characterized by N_2 (77 K) adsorption using a BELSORP-mini II adsorption apparatus (Japan). The BET surface area was measured from the adsorption isotherms using Brunauer–Emmett–Teller equation. The Dubinin–Radushkevich (DR) equation was used to calculate the micropore volume. The total volume (V_t) was obtained at a relative pressure of 0.99. Pore size distribution was obtained from Horvath-Kawazoe (HK) analysis. Prior to the measurement, the samples were degassed at 393 K for 12 h in the degas port of the apparatus.

The elemental composition of palm shell activated carbon and the modified activated carbons were obtained by a CHNS/O analyzer (PE2400 Series II, Perkin-Elmer, USA). Images of the adsorbent surfaces were investigated by Scanning Electron Microscope (SEM, LEO 1455 VP, United Kingdom). Functional groups on the material surfaces were investigated by FTIR Spectrometer (Perkin Elmer, System 2000R, USA). The KBr compression method was used for preparing samples for FTIR analysis. Each sample was ground together with potassium bromide (KBr) to fine powder and the mixture was pressed by a hydraulic press to form a KBr pellet. The zeta potentials were determined by laser droppler electrophoresis using a Zetasizer (Nanoseries ZS model S4700, Malvern Instrument, UK). Thermogravimetric Analyses (Perkin Elmer, Thermogravimetric Analyzer TGA 7, USA) was used to assess the mass change, or thermal degradation, of the native and the modified activated carbon as a function of temperature.

2.4 *Adsorption analysis*

2.4.1 Apparatus

The experimental apparatus used in both the static and dynamic adsorption was previously reported in Phalakornkule [13]. The main components of the apparatus were a single stainless steel column with a diameter of 1.9 cm, height of 80 cm and total volume of 200 cm^3 packed containing 160 g of the adsorbent. The column was equipped with three automatic solenoid valves (SV1-SV3). SV1 controlled the feed stream, SV2 the raffinate stream and SV3 the extract stream. Two temperature detectors were positioned at the column inlet and outlet to measure any temperature variation due to the adsorption process. Two flowmeters (Dwyer, measuring ranges 0–10 L/min at STP and 0–5 L/min at STP) was installed at the inlet and outlet to record the flow rate and a pressure gauge (a maximum pressure of 10^3 kPa) was installed at the column to measure the pressure variation. A vacuum pump (30 kPa, GAST Manufacturing Corp., USA) was employed to desorb the gas before and after each experiment.

2.4.2 Static Adsorption

The one column pressure swing adsorption system was used for static volumetric gas adsorption. First, valve SV3 was opened, while the other valves were closed, allowing the system to be evacuated. When the necessary vacuum was achieved, valve SV1 was opened momentarily, allowing the gas to flow from the feed tank until the adsorption pressure of 400 kPa was achieved. The flow rate was measured by the flowmeter and the total quantity of feed gas can be determined from the ideal gas law:

$$n_{feed} = \frac{P_{ads} \int \dot{V}_t dt}{RT} \quad (2)$$

where P_{ads} is the feed pressure (Pa or bar), $\dot{V}_t$ is the volumetric flow rate at an instantaneous time (m^3/s or L/min), t is the time that the valve SV1 is opened

(s or min), R is the universal gas constant (8.314 m^3·Pa/mol·K or 0.08314 L·bar/mol·K), T is the operating temperature (K) and n_{feed} is the total quantity of feed gas (mole).

Pressure drop was monitored during the adsorption process in which some quantity of gas was adsorbed by the adsorbent and was removed from the gas phase. As the equilibrium pressure (P_e) was achieved, the quantity of gas (n_e) remaining in the gas phase can be calculated from the ideal gas law:

$$n_e = \frac{P_e V_{column}}{RT} \quad (3)$$

where P_e is the equilibrium pressure (Pa or bar), V_{column} is the column volume accounting for the true volume of the adsorbent sample (m^3 or L), R is the universal gas constant (8.314 m^3·Pa/mol·K or 0.08314 L·bar/mol·K), T is the operating temperature (K) and n_e is the quantity of gas remaining in the gas phase (mole).

Once n_e was determined, the quantity of gas adsorbed (n_{ads}) by the sample at P_e can be calculated as follow:

$$n_{ads} = n_{feed} - n_e \quad (4)$$

This established a point on an isotherm. After that, valve SV3 was opened while the other valves were closed to desorb the gas from the adsorbent sample. The process was repeated for other P_e by dosing higher n_{feed} which can be obtained by using higher feed flow rates. The process was repeated until the analysis pressure was near saturation pressure.

The modified activated carbon samples were subjected to adsorption of CO_2, H_2 and N_2. Equilibrium selectivity for a binary gas was obtained by the ratio of maximum equilibrium adsorption capacity of each gas on the same adsorbent sample.

2.4.3 Dynamic adsorption

The dynamic adsorption was carried out by passing the standard gas mixtures (50/30/20% $CO_2/H_2/N_2$ v/v) through the adsorption column at 298 K. The controlled room temperature was chosen because most of the pressure swing adsorption (PSA) systems were operated at an ambient condition [2]. Before each experiment, the gas was evacuated to 30 kPa by the vacuum pump during the vacuum step. The three-step adsorption cycle was operated: 1) pressurization, 2) adsorption and 3) depressurization, via three automatic solenoid valves operated according to Phalakornkule *et al*. [13].

The pressure during the pressurization and adsorption steps was 400 kPa. The feed flow rate during the pressurization step was 2 L/min at STP for 2 min. During the adsorption step, the system was holding constant for 15 min to ensure that equilibrium was achieved. During the depressurization, the gas exits at the end of the column and the gas composition was determined by a gas chromatograph (GC) equipped with a thermal conductivity detector (GC-2014; SHIMADZU, Japan), a stainless steel packed column and an argon carrier gas with a flow rate of 50 mL/min. During the depressurization step, the gas was desorbed by a reduction in pressure from the adsorption pressure to atmospheric pressure. The cycle was repeated until a breakthrough of CO_2 was reached.

2.5 *Data analysis*

In this study, the measurements were repeated three times. The standard errors were all within 10% of the mean value. A test of significant difference based on the paired *t*-statistic was performed using the Excel Solver Add-in. The difference was regarded as not significant if the paired t-statistic showed probability; $P > 0.05$ and significant if $P < 0$ .05.

3 Results

3.1 *Comparative characteristics of the native and modified activated carbon*

A series of percentage weights of chitosan on the activated carbon, 0.12, 0.25, 0.56, 0.66 and 0.76 wt%, was obtained from the impregnation of the AC in the 50 mL chitosan solution with initial concentrations between 0.1, 0.5, 1.0, 1.5 and 2.0 g/L. The amount of chitosan impregnated on the activated carbon was relatively high, compared to the amount of polyethyleneimine (PEI) on activated carbon [12]. The adsorption of PEI molecules with average molecular weight between 600,000–1,000,000 g/mol was approximately 0.26 wt%. A possible explanation was that the large molecular size of PEI prohibited infiltration into most of the micropores of the activated carbon with almost 100% microporous.

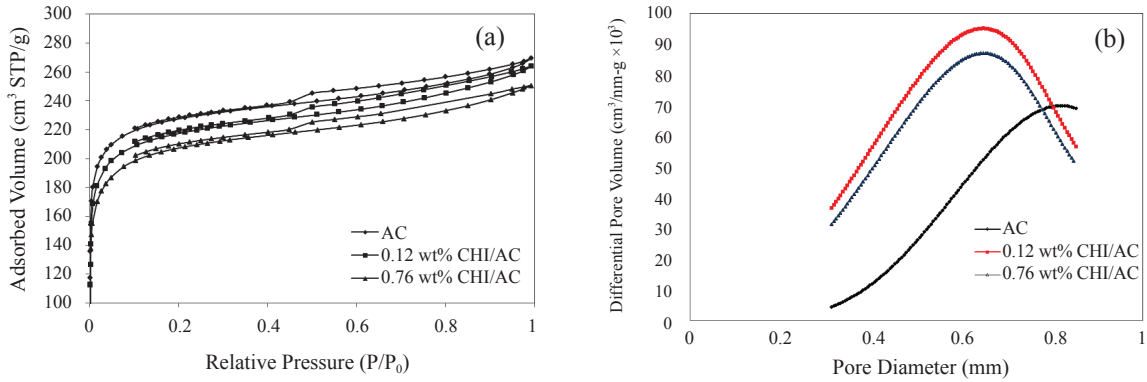

Figure 1: Surface characteristics of the native and modified activated carbons (a) adsorption-desorption isotherm (b) pore size distribution.

Table 2: Surface characteristics and elemental composition of the native and the chitosan impregnated activated carbon

Samples	BET Surface Area[a] (m^2/g)	Micropore Volume[b] (cm^3/g)	Mean Pore Diameter (nm)	Total Pore (cm^3/g)	Element Analysis			
					C	H	N	Other
AC	868.29	199.49	1.9182	0.4164	70.02	1.33	0.00	28.18
0.12 wt% CHI/AC	840.79	193.18	1.9414	0.4081	-	-	-	-
0.25 wt% CHI/AC	764.06	175.55	1.9109	0.3650	-	-	-	-
0.56 wt% CHI/AC	764.83	175.72	2.0363	0.3873	-	-	-	-
0.66 wt% CHI/AC	786.01	180.59	2.1144	0.4155	-	-	-	-
0.76 wt% CHI/AC	760.70	174.77	1.8915	0.3617	70.32	2.91	0.41	26.31

Remarks: [a] Multi-point BET surface area using N_2 as adsorptive gas; [b] Micropore volume was calculated by Dubinin-Radushkevish (D-R) method

Figure 1(a) shows the adsorption-desorption isotherms of the native activated carbon and 0.12 wt% and 0.76 wt% CHI/AC. The isotherm of the native activated carbon is of type IV according to the IUPAC classification. Type IV isotherms describe adsorption in mixed situations of micropores and mesopores [18]. A hysteresis loop can be found when the mechanism of filling by capillary condensation in mesopores differs from that of mesopore emptying. The activated carbon with a significant mesopore volume may be suitable for the impregnation by large molecules like chitosan because this large molecular weight biopolymer may not be able to penetrate into the micropores easily due to steric effects. The molecular weight average and molecular weight distribution of the oligomer chitosan in this study were found to be 17,010 Da and 5.48, respectively. Therefore, mesopores should have a significant contribution to the impregnation process. It can be observed from Figure 1(a) that the chitosan impregnated samples had the lower N_2 adsorption than the native activated carbon, suggesting that some adsorption areas were lost due to the impregnation.

Figure 1(b) shows the pore size distributions of the native activated carbon and 0.12 wt% and 0.76 wt% CHI/AC. With the chitosan impregnation onto the native activated carbon, the peaks of the pore size distribution curves of 0.12 wt% and 0.76 wt% CHI/AC shifted to the left, indicating that some of the micropore mouths narrowed down and more ultra micropores (< 0.7 nm) were developed.

Table 2 reports the surface characteristics of the native and the impregnated activated carbon. It is evident that the BET surface area and the micropore volume of the modified activated carbon were reduced by the impregnation process. For the 0.12 wt% CHI/AC, the BET surface area marginally decreased by 3% indicating that a slight portion of the micropores was blocked. Chitosan impregnation at higher ratios of 0.25%, 0.56%, 0.66% and 0.76% led to the BET surface area reduction by 12%, 12%, 9.5% and 12.4%, respectively. The reduction in nitrogen adsorption was due to excess constriction of pore size in the samples

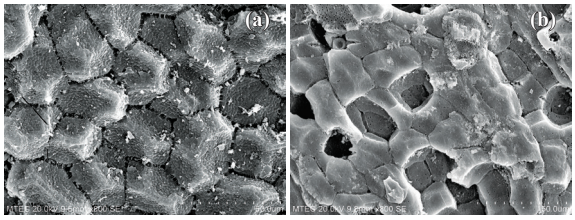

Figure 2: SEM images of the native activated carbon (a) and the 0.12 wt% chitosan impregnated activated carbon (b) (X 800 magnification).

rendering reduced accessibility of nitrogen molecule into the inner pores. Chitosan impregnation was also evident from the elemental analysis. In the case of the native activated carbon, the percentages of hydrogen and nitrogen were relatively low. In contrast, the hydrogen and nitrogen content in the chitosan impregnated samples were significantly higher. The hydrogen content increased from 1.33% for the native to 2.91% for the 0.76 wt% CHI/AC, while the nitrogen content increased from nil to 0.41%. The measured elemental compositions were closed to the elemental compositions calculated based on the percentage weight of chitosan on AC and the elemental compositions of AC and chitosan.

The surface morphologies of the native and the chitosan impregnated activated carbon were compared using SEM at X 800 magnification. The order of this magnification was not high enough to observe the pore structure on the native activated carbon [Figure 2(a)]. However, the coverage of chitosan on the surface of the impregnated activated carbon can be observed from the SEM image shown in Figure 2(b).

FTIR spectra were collected for qualitative characterization of surface functional groups of the activated carbon before and after the impregnation with chitosan. Figure 3 shows the comparative FTIR spectra of chitosan, the native activated carbon and the chitosan impregnated activated carbon. The IR assignments of functional groups were performed using the information in the literature (Table 3). The characteristic bands of chitosan can be observed at 3363, 1658, 1598, 1423, 1384 and 1323 cm^{-1} which can be attributed to $–NH_2$ and –OH groups stretching vibration and amide I (N-acetyl glucosamine units), N–H angular deformation (N-acetyl glucosamine amide II), C–N axial deformation of the amino groups, CH_3 symmetrical angular deformation and C–N axial

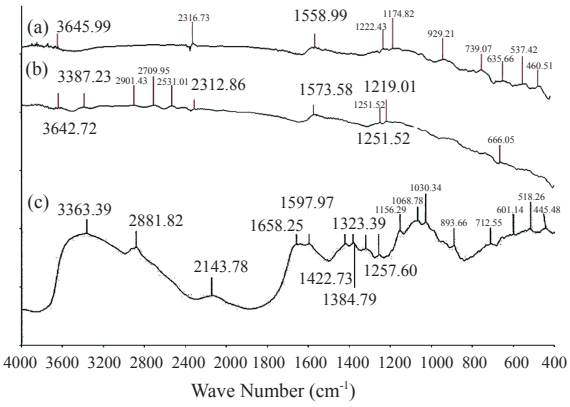

Figure 3: FTIR spectra of the chitosan and the native and the 0.12 wt% chitosan impregnated activated carbon.

deformation of the amino groups, respectively [19], [20].

Table 3: Possible FTIR peak assignments for the functional groups on the chitosan and the native and chitosan impregnated activated carbon

Group of Functionality	Wave Number Assignments (cm^{-1})	References
alcohols O-H	~3600	[21]
phenolic groups O-H C-OH	 ~3390 1400-1000	[22], [25]
carboxylic acids	3300-2500	[23]
ring vibration in a large aromatic skeleton	1590-1500	[22], [24]
$–NH_2$ and –OH groups stretching vibration	~3449	[19]
amide I band (N-acetyl glucosamine units)	~1650	[20]
N–H angular deformation (N-acetyl glucosamine amide II)	~1565, ~1570	[20]
CH_3 symmetrical angular deformation	~1386	[20]
C–N axial deformation of the amino groups	~1411	[20]
C–N axial deformation of the amino groups	~1324	[20]

The FTIR spectra of the native activated carbon displays absorption bands at 3643 cm^{-1}, 3387 cm^{-1}, 3000–2500 cm^{-1} which can be assigned as O-H in alcohols, O-H in phenols and carboxylic acids, respectively [21]–[23]. The band around 1590–1500 cm^{-1}

is assigned to ring vibration in a large aromatic skeleton generally found in carbonaceous material, such as activated carbon [22], [24]. The absorption bands at 1400–1000 cm^{-1} can be assigned as C-O bonds stretching modes [25]. The FTIR spectra of the chitosan impregnated activated carbon were similar to the native activated carbon. The characteristic bands of chitosan cannot be observed because the amount of impregnated chitosan was less than 1%. However, it can be noticed that the bands assigned for carboxylic acids disappeared and the disappearance of the band could be attributed to the linkage between the carboxylicions on the activated carbon surfaces and the ammonium ions of chitosan. This explanation was supported by the zeta potential values of the activated carbon before and after the impregnation with chitosan.

The intrinsic pKa of chitosan is closed to 6.5 [26], therefore most amine groups were protonated under the condition of the impregnation (pH 3–4). The zeta potential measurement revealed that the native activated carbon had slightly negative surface charges [–6 mV on an average, Figure 4(a)]. Consequently, attractive electrostatic interactions were the important forces that lead to the assembly of chitosan onto the activated carbon surfaces. The zeta potential measurement revealed that the chitosan impregnated activated carbon had high positive zeta potential [36 mV on an average, Figure 4(b)].

The temperature effect on the activated carbon and impregnated activated carbon was investigated using thermogravimetric analysis (TGA). The TGA profiles obtained under inert gas condition are shown in Figure 5. The first weight loss around 373 K was observed for the native activated carbon. The weight loss was probably caused by thermal desorption of physically adsorbed material such as water vapor, hydrocarbon and residual volatile content [27]. The second weight loss was observed when the temperature reached 873 K and gradual and pronounced weight loss was continued up to 1273 K. In the latter case, the weight loss was caused by volatile lumps and structure disruption of the native activated carbon.

In the case of the impregnated activated carbon, the first weight loss was occurred at the same temperature as of the native activated carbon around 373 K. However, the second weight loss occurred at the temperature range 423–473 K. The second weight loss was probably caused by thermal desorption of

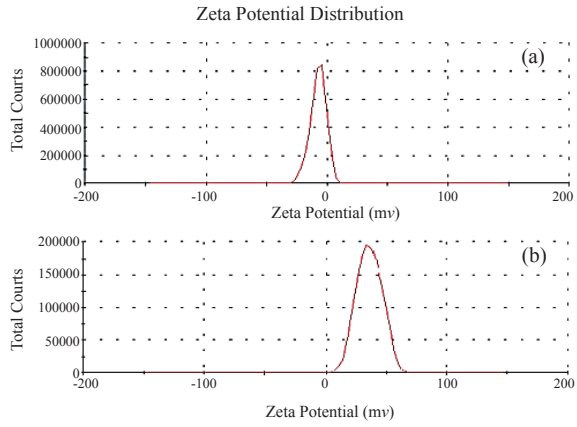

Figure 4: Zeta potential of (a) the native activated carbon (b) the 0.12 wt% chitosan impregnated activated carbon.

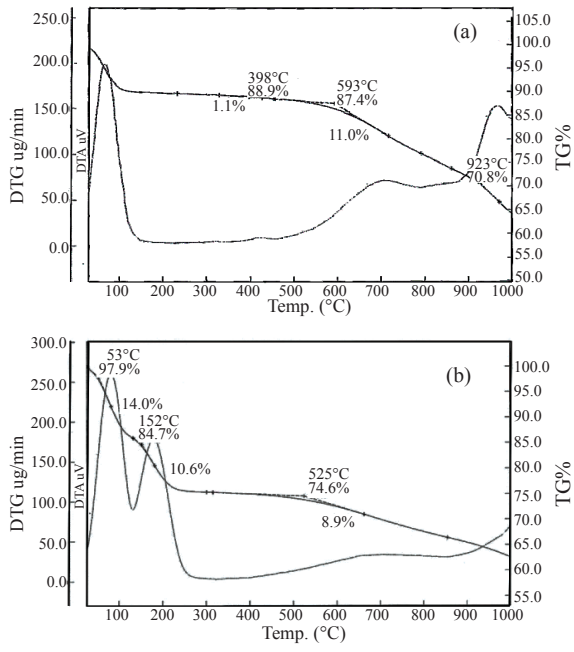

Figure 5: TGA curves (a) the native activated carbon (b) the 0.12 wt% chitosan impregnated activated carbon.

functional groups of chitosan. Similar to the native activated carbon, the final weight loss was observed when the temperature reached 873 K and gradual and pronounced weight loss was continued up to 1273 K. The TGA suggested that the temperature for regenerating the chitosan impregnated samples should be below 473 K.

3.2 *Adsorption and equilibrium selectivity at PSA operating pressure*

In most previous studies, adsorption and equilibrium selectivity were investigated at low range pressures (200–800 mm Hg or 26–105 kPa) using a commercial volumetric adsorption system [13], [28], [29]. However, in practice, gas separation by pressure swing adsorption is performed at higher pressures (>400 kPa). Furthermore, it is reported in the literature that ideal selectivity of CO_2/CH_4 and CO_2/N_2 drops significantly from 25 to 3.5 and from 50 to 7 when pressure is increased from 20 kPa to 400 kPa [30]. Therefore, in this study, the adsorption and equilibrium selectivity were investigated at a high pressure range of 400 kPa.

Figure 6(a) and Figure 6(b) shows the adsorption profiles of carbon dioxide and hydrogen on the native and chitosan impregnated activated carbons. The 0.12 wt% CHI/AC was found to have 11% higher CO_2 adsorption capacity than the native activated carbon even though its surface area was reduced by 3% due to the impregnation process. Chitosan may help enhance adsorption of CO_2 by means of chemical interactions between its surface and CO_2. The enhanced adsorption of CO_2 can be attributed to increased nitrogen functional groups on surface of activated carbon. The mechanism of CO_2 chemical adsorption is shown in equation (5). Two moles of amine groups react with 1 mole of CO_2 molecule.

$$CO_2 + 2RNH_2 \leftrightarrow NH_4^+ + R2NCOO^- \quad (5)$$

This contribution was in a similar fashion as that by impregnation of PEI onto activated carbon [9]–[11]. The experimental data shows that the 0.12 wt% chitosan impregnation enhanced CO_2 adsorption by chemisorptions via reaction with numerous amine group adsorption sites.

As shown in Figure 6(a), the modified activated carbon with the higher ratios of 0.25%, 0.56%, 0.66% and 0.76% had the lower CO_2 adsorption capacity than the native activated carbon. The BET surface area analysis indicated that excess constriction of pore size occurring in these samples rendering reduced accessibility of nitrogen molecule into the inner pores. Since the kinetic diameters of carbon dioxide and nitrogen are comparable: 3.30 Å for carbon dioxide and 3.64 Å for nitrogen [31]–[33], the reason for the reduction in CO_2 adsorption capacity was speculated to be the same as that for N_2 adsorption capacity. It is known that hydrogen hardly adsorbed on carbon materials under typical operating pressures (< 10 MPa) [33] and the H_2 adsorption capacities were found to be the same at 0.32 mole per kg adsorbent for all samples under the investigation [Figure 6(b)].

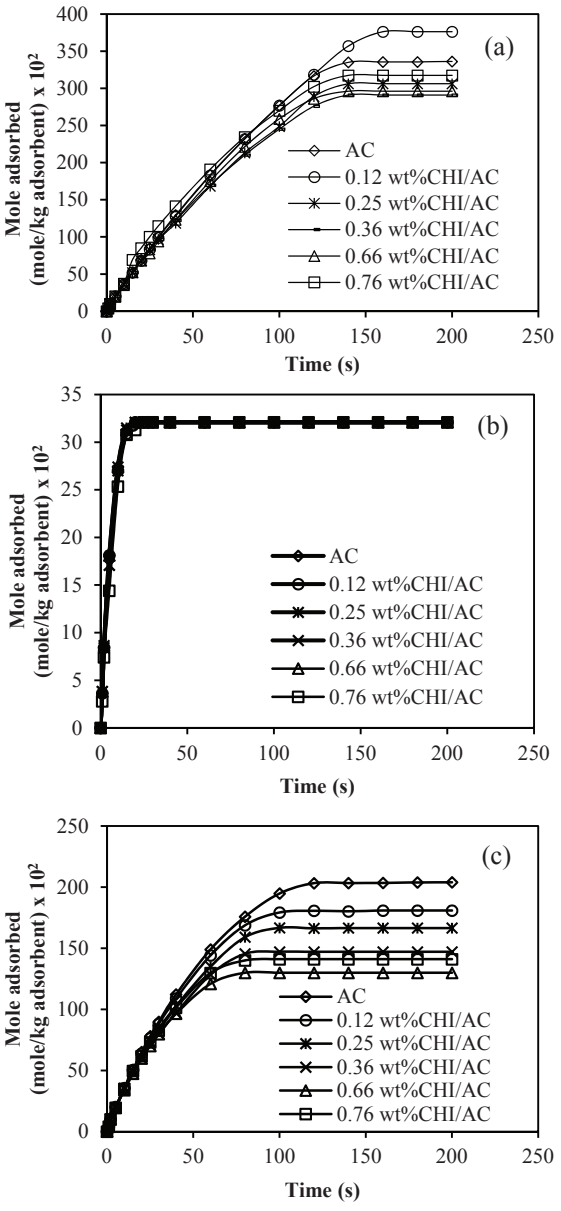

Figure 6: Adsorption profile of the native and chitosan impregnated activated carbon (a) CO_2 adsorption, (b) H_2 adsorption and (c) N_2 adsorption.

The pure component selectivity of CO_2/H_2 calculated from the ratio of the equilibrium adsorption of each gas on the same adsorbent at 298 K and 400 kPa was 10.53, 11.72, 9.54, 9.07, 9.22, 9.90 for the native activated carbon, 0.12, 0.25, 0.56, 0.66 and 0.76 wt% CHI/AC, respectively.

3.3 *Isotherm models*

The hydrogen and nitrogen adsorption data (Figure 6(b) and Figure 6(c)) was fitted with Toth isotherm model according to equation (6) and the carbon dioxide adsorption data [Figure 6(a)] was fitted with Multisite Langmuir isotherm model according to equation (7).

$$q_i = q_{mi} \frac{K_i P}{[1+K_i P]^{\frac{1}{n_i}}} \quad (6)$$

$$K_i = K_i^0 exp\left[-\frac{\Delta H_i}{RT}\right] \quad (7)$$

$$n_i = A_i + B_i T \quad (8)$$

where q_i is the absolute amount adsorbed of component i (mol/kg). q_{mi} is the maximum amount adsorbed of component i (mol/kg). K_i^0 is the infinite adsorption constant (bar^{-1}). K_i is adsorption constant (bar^{-1}). P is pressure (bar). ΔH_i is the isosteric heat of adsorption (kJ/mol). n_i is the heterogeneity parameter. A_i, B_i are the parameters relating the thermal variation of the heterogeneity coefficient (-, K^{-1}).

$$\frac{q_i}{q_{mi}} = K_i P \left(1-\frac{q_i}{q_{mi}}\right)^{a_i} \quad (9)$$

where a_i is the number of neighboring sites occupied by component i. K_i is the equilibrium constant as in equation (7) (bar^{-1}).

Table 4 and 5 reports the parameters in Toth and Multisite Langmuir isotherm models for the adsorption of H_2, N_2 and CO_2 on the native activated carbon and the chitosan impregnated activated carbon, respectively. It can be seen that the Toth model was suitable for the H_2 and N_2 adsorption, while the Multisite Langmuir isotherm model was suitable for fitting the CO_2 adsorption with R^2 between 0.995–1.000.

Table 4: Parameters in Toth isotherm models for the adsorption of H_2 and N_2 on the native activated carbon and the chitosan impregnated activated carbon

Sample	Gas Species	q_m mol•kg^{-1}	K_i MPa^{-1}	-ΔHi kJ•mol^{-1}	A_i	B_i K^{-1}	R^2
AC	N_2	18.28×10^{9}	1.13×10^{-6}	8.63×10^{-7}	1.43×10^{-6}	0.0002	0.995
	H_2	28.06	1.04	2.01×10^{-6}	53.80	0.1801	0.999
0.12 wt% CHI/AC	N_2	785.56	1.57	2.99×10^{-6}	0.73	0.0011	0.996
	H_2	32.61	1.45	3.97×10^{-7}	1.86	0.0047	1.000
0.25 wt% CHI/AC	N_2	16.75×10^{9}	3.09×10^{-7}	3.13×10^{-6}	2.45×10^{-13}	0.0003	0.993
	H_2	26.78	1.82	3.97×10^{-7}	1.97	0.005	1.000
0.56 wt% CHI/AC	N_2	230.25	0.94	3.02×10^{-6}	1.29	0.0008	0.999
	H_2	26.78	1.81	3.97×10^{-7}	1.97	0.005	1.000
0.66 wt% CHI/AC	N_2	11.35×10^{9}	4.00×10^{-6}	2.86×10^{-6}	1.51×10^{-8}	0.0002	0.997
	H_2	27.2727	2.83	3.97×10^{-7}	1.75	0.0043	1.000
0.76 wt% CHI/AC	N_2	12.42×10^{9}	6.01×10^{-8}	3.12×10^{-6}	4.47×10^{-13}	0.0003	0.996
	H_2	29.18	1.97	3.97×10^{-7}	1.75	0.0043	1.000

Table 5: Parameters in Multisite Langmuir isotherm models for the adsorption of CO_2 on the native activated carbon and the chitosan impregnated activated carbon

Sample	Gas Species	q_m mol•kg^{-1}	K_i MPa^{-1}	-ΔHi kJ•mol^{-1}	a_i	R^2
AC	CO_2	819.8	0.0020	2.84×10^{-6}	9.35	0.974
0.12 wt% CHI/AC	CO_2	457.3	0.0076	∞	0.062	0.994
0.25 wt% CHI/AC	CO_2	380.0	0.0111	5.77×10^{-6}	5.78×10^{-6}	0.992
0.56 wt% CHI/AC	CO_2	373.2	0.0243	3.49×10^{-6}	3.49	0.977
0.66 wt% CHI/AC	CO_2	387.4	0.0019	1.24×10^{-5}	36.22	0.973
0.76 wt% CHI/AC	CO_2	395.5	0.0164	2.30×10^{-5}	4.87	0.992

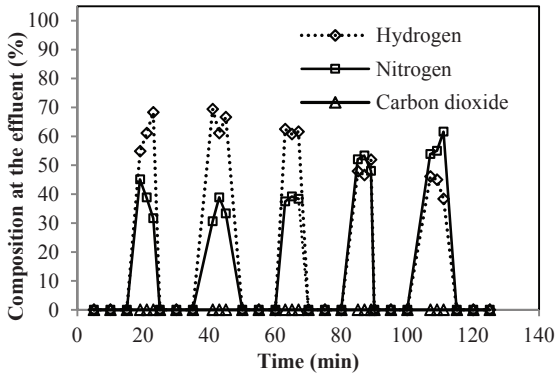

Figure 7: Dynamic adsorption separation of 50-30-20 mixture of $CO_2/H_2/N_2$ on the 0.12 wt% CHI/AC.

3.4 *Dynamic adsorption*

In our previous study [13], the binary adsorption dynamics of the activated carbon bed was investigated by feeding CO_2/H_2 gas mixture (50:50 v/v) to the adsorption system. It was evident that the 0.12 wt% CHI/AC adsorbed carbon dioxide more effectively, leading not only to the higher H_2 purity at the early cycles, but also the longer effective operating cycles. When using the native activated carbon as the adsorbent, high purity hydrogen in the range of 93–100% was achieved during cycle 1–3. However, during cycle 4–7, the hydrogen purity dropped significantly to the range of 72–84%. When using the 0.12 wt% CHI/AC as the adsorbent, 100% hydrogen was achieved during cycle 1–8, and the breakthrough of CO_2 occurred at cycle 9 with a relatively steep concentration profile.

In this study, the tertiary adsorption dynamics of the activated carbon bed was investigated by feeding $CO_2/H_2/N_2$ gas mixture (50:30:20 v/v) to the adsorption system for 5 cycles. It was found that H_2 and N_2 were the only components in the gas effluent, and there was no CO_2 detected in the effluent stream for the entire operation (see Figure 7). The results suggested that the chitosan impregnated activated carbon was effective in separating CO_2 from the tertiary gas mixture as in the binary gas mixture.

4 Discussion

In contrast to physical adsorption of CO_2 onto the native activated carbon, chemisorptions is the underlying mechanism for CO_2 adsorption onto the chitosan impregnated activated carbon and desorption of carbon dioxide from the modified adsorbent requires heat regeneration.

The study of carbon dioxide capture during hydrogen processes has gained growing attention by researchers worldwide. CO_2 capture has been coupled with hydrogen production via steam gasification of biomass [34], steam reforming of natural gas [35], [36], pyrolysis of biomass [37], integrated gasification combined cycle [38] and coal gasification [39]. For these applications, the desired sorbent must be able to adsorb/absorb CO_2 at relatively high temperatures. In most cases, Ca-based materials such as CaO [34], [37], a mixture of CaO and $CaCO_3$ [36] have been employed. In the study by Wang *et al*. (2008, [40]), Ca_2SiO_4 was synthesized from $CaCO_3$ and SiO_4 which can absorb CO_2 at a broad temperature gap ranging from 773–1073 K.

In this study, the purification of biohydrogen by separating carbon dioxide from hydrogen can lead to the integration between high purity hydrogen production and carbon dioxide capture and storage. In a process that aims for purifying biohydrogen alone, three factors are considered for an ideal adsorbent: 1) high adsorption capacity 2) high selectivity for carbon dioxide and 3) the easiness for adsorbent regeneration. Therefore, the affinity of an adsorbent for carbon dioxide should not be too high in that case; otherwise the regeneration step will negatively affect the economy of the process. However, for an integrated process of both hydrogen purification and carbon dioxide capture and storage, regeneration of the adsorbent may not be necessary as the adsorbent also works as carbon storage, but the affinity of an adsorbent for carbon dioxide should be maximized. The modified activated carbon developed in this study would serve this purpose because it has higher adsorption capacity and higher carbon dioxide selectivity compared to the native activated carbon without modification. The maximum of 3.76 mole of CO_2 adsorbed per kg of the chitosan impregnated activated carbon [see Figure 6(a)] was found to be comparable with the maximum of 3.39 mole of CO_2 adsorbed per kg of CaO during carbonation [36].

5 Conclusions

Chitosan impregnated activated carbon was successfully prepared by immersing palm shell activated carbons

in the chitosan solutions under agitation. The zeta potential measurement revealed that while the native activated carbon had slightly negative surface charges (–6 mV), the chitosan impregnated activated carbon had high positive zeta potential (36 mV). Besides the surface charge property, the BET surface areas and pore size distributions were significantly affected by the impregnated chitosan. The use of chitosan impregnation to modify the palm shell based activated carbon can enhance both CO_2 adsorption capacity and high selectivity for CO_2. The maximum of 3.76 mole of CO_2 adsorbed per kg of the chitosan impregnated activated carbon at 400 kPa and 298 K was achieved. In addition to the static adsorption, the dynamic adsorption of 50-30-20 mixture of CO_2-H_2-N_2 by the chitosan impregnated activated carbon showed nil concentration of CO_2 at the effluent for at least 5 cycles.

Acknowledgments

The authors would like to acknowledge the National Research Council of Thailand for the research funding (2553A11902006 and 2555A11902006) that made the investment of valuable research units and operations possible. The research work is partially supported by the advancing research fund of King Mongkut's University of Technology North Bangkok (KMUTNB). We would like to thank Taming Enterprises Co., Ltd. for providing chitosan samples.

References

[1] X. Chen, Y. Sun, Z. Xiu, X. Li, and D. Zhang, "Stoichiometric analysis of biological hydrogen production by fermentative bacteria," *International Journal of Hydrogen Energy*, vol. 31, no. 4, pp. 539–549, 2006.

[2] M. R. Douglas, S. Farooq, and K. S. Knaebel, *Pressure Swing Adsorption*. USA, New York: VCH, 1994.

[3] J. P. Boudou, M. Chehimi, E. Broniek, T. Siemieniewska, and J. Bimer, "Adsorption of H_2S or SO_2 on an activated carbon cloth modified by ammonia treatment," *Carbon*, vol. 41, no. 10, pp. 1999–2007, 2003.

[4] J. Jaramillo, P. M. Álvarez, and V. Gómez-Serrano, "Oxidation of activated carbon by dry and wet methods, surface chemistry and textural modifications," *Fuel Processing Technology*, vol. 91, no. 11, pp. 1768–1775, 2010.

[5] A. Heidari, H. Younesi, A. Rashidi, and A. A. Ghoreyshi, "Adsorptive removal of CO_2 on highly microporous activated carbons prepared from Eucalyptus camaldulensis wood: Effect of chemical activation," *Journal of the Taiwan Institute of Chemical Engineers*, vol. 45, no. 2, pp. 579–588, 2014.

[6] H. Cui, S. Q. Turn, and M. A. Reese, "Removal of sulfur compounds from utility pipelined synthetic natural gas using modified activated carbons," *Catalysis Today*, vol. 139, no. 4, pp. 274–279, 2009.

[7] J. Wei, L. Liao, Y. Xiao, P. Zhang, and Y. Shi, "Capture of carbon dioxide by amine-impregnated as-synthesized MCM-41," *Journal of Environmental Sciences*, vol. 22, no. 2, pp. 1558–1563, 2010.

[8] P. D. Jadhav, R. V. Chatti, R. B. Biniwale, N. K. Labhsetwar, S. Devotta, and S. S. Rayalu, "Monoethanol amine modified zeolite 13X for CO_2 adsorption at different temperatures," *Energy & Fuels*, vol. 21, no. 6, pp. 3555–3559, 2007.

[9] D. P. Bezerra, R. S. Oliveira, R. S. Vieira, C. L. Cavalcante Jr., and D. C. S. Azevedo, "Adsorption of CO_2 on nitrogen-enriched activated carbon and zeolite 13X," *Adsorption-Journal of the International Adsorption Society*, vol. 17, no. 1, pp. 235–246, 2011.

[10] A. Heydari-Gorji and A. Sayari, "CO_2 capture on polyethylenimine-impregnated hydrophobic mesoporous silica: Experimental and kinetic modeling," *Chemical Engineering Journal*, vol. 173, no. 1, pp. 72–79, 2011.

[11] A. Zhao, A. Samanta, P. Sarkar, and R. Gupta, "Carbon dioxide adsorption on amine-impregnated mesoporous SBA-15 sorbents: Experimental and kinetics study," *Industrial & Engineering Chemistry Research*, vol. 52, no. 19, pp. 6480–6491, 2013.

[12] C.-H. Yu, C.-H. Huang, and C.-S. Tan, "A review of CO_2 capture by absorption and adsorption," *Aerosol and Air Quality Research*, vol. 12, pp. 745–769, 2012.

[13] C. Phalakornkule, J. Foungchuen, and T. Pitakchon, "Impregnation of chitosan onto activated carbon for high adsorption selectivity towards CO_2: CO_2 capture from biohydrogen, biogas and flue gas,"

Journal of Sustainable Energy & Environment, vol. 3, no. 4, pp. 153–157, 2012.

[14] G. M. Hall, "Biotechnology approaches to chitin recovery," in *Proceedings of 2nd Asia Pacific Symposium*, Bangkok, Thailand, 1996, pp. 26.

[15] W. F. Stevens, "Chitosan: A key compound in biology and bioprocess technology," in *Proceedings of 2nd Asia Pacific Symposium*, Bangkok, Thailand, 1996, pp. 13.

[16] W. F. Stevens, "Production of chitin and chitosan: Refinement and sustainability of chemical and biological processing," in *Proceedings of 8th International Chitin and Chitosan Conference and 4th Asia Pacific Chitin and Chitosan Symposium*, Yamaguchi, Japan, 2000, pp. 293.

[17] E. R. Hayes, D. H. Davies, and V. G. Munroe, "Organic solvent systems for chitosan," in *Proceedings of 1st International Conference on Chitin and Chitosan*, MIT Sea Grant Program, Massachusetts, USA, Edited by Muzzarelli RAA, Pariser ER., 1977, pp. 103.

[18] R. F. P. M. Moreira, H. J. José, and A. E. Rodrigues, "Modification of pore size in activated carbon by polymer deposition and its effects on molecular sieve selectivity," *Carbon*, vol. 39, no. 15, pp. 2269–2276, 2001.

[19] D. R. Bhumkar and V. B. Pokharkar, "Studies on effect of pH on cross-linking of chitosan with sodium tripolyphosphate: a technical note," *AAPS PharmSciTech*, vol. 7, no. 2, E138–E143, 2016.

[20] D. Ghosh, A. Pramanik, N. Sikdar, S. K. Ghosh, and P. Pramanik, "Amelioration studies on optimization of low molecular weight chitosan nanoparticle preparation, characterization with potassium per sulphate and silver nitrate combined action with aid of drug delivery to tetracycline resistant bacteria," *International Journal of Pharmaceutical Sciences and Drug Research*, vol 2, no. 4, pp. 247–253, 2010.

[21] J. McMurry, *Organic Chemistry*, 3rd ed., USA, California: Brooks/Cole, 1992, pp. 435.

[22] V. Sricharoenchaikul, C. Pechyen, D. Aht-ong, and D. Atong, "Preparation and characterization of activated carbon from the pyrolysis of physic nut (*Jatropha curcas* L.) waste," *Energy & Fuels*, vol. 22, no. 1, pp. 31–37, 2008.

[23] W. Shen, Z. Li, and Y. Liu, "Surface chemical functional groups modification of porous carbon," *Recent Patents on Chemical Engineering*, vol. 1, no. 1, pp. 27–40, 2008.

[24] R. C. Sun and J. Tomkinson, "Fraction separation and physic-chemical analysis of lignin from the black liquor of oil palm trunk fibre pulping," *Separation and Purification Technology*, vol. 24, pp. 529–539, 2001.

[25] A. S. Shafeeyan, W. M. A. W. Daud, A. Houshmand, and A. Shamiri, "A review on surface modification of activated carbon for carbon dioxide adsorption," *Journal of Analytical and Applied Pyrolysis*, vol. 89, no. 2, pp. 143–151, 2010.

[26] C. Kaseamchochoung, P. Lertsutthiwong, and C. Phalakornkule, "Influence of chitosan characteristics and environmental conditions on flocculation of anaerobic sludge," *Water Environment Research*, vol 78, no. 11, pp. 2210–2216, 2006.

[27] A. Kongnoo, P. Intharapat, P. Worathanakul, and C. Phalakornkule, "Diethanolamine impregnated palm shell activated carbon for CO_2 adsorption at elevated temperatures," *Journal of Environmental Chemical Engineering*, vol. 4, no. 1, pp. 73–81, 2016.

[28] J. S. Tan and F. N. Ani, "Carbon molecular sieved produced from oil palm shell for air separation," *Separation and Purification Technology*, vol. 35, pp. 47–54, 2004.

[29] R. S. Pillai, S. A. Peter, and R. V. Jasra, "Adsorption of carbon dioxide, methane, nitrogen, oxygen and argon in NaETS-4," *Microporous and Mesoporous Materials*, vol. 113, no. 1–3, pp. 268–76, 2008.

[30] S. Cavenati, C. A. Grande, and A. E. Rodrigues, "Adsorption equilibrium of methane, carbon dioxide, and nitrogen on zeolite 13X at high pressures," *Journal of Chemical and Engineering Data*, vol. 49, no. 4, pp. 1095–1101, 2004.

[31] D. W. Breck, *Zeolite Molecular Sieves*. USA, Florida: Krieger Publishing Company, 1984, pp. 636.

[32] S. Sircar, "Basic research needs for design of adsorptive gas separation processes," *Industrial & Engineering Chemistry Research*, vol. 45, no. 16, pp. 5435–5448, 2006.

[33] R. Ströbel, L. Jörissen, T. Schliermann, V. Trapp, W. Schütz, K. Bohmhammel, G. Wolfand, and

J. Garche, "Hydrogen adsorption on carbon materials," *Journal of Power Sources*, vol. 84, no. 2, pp. 221–224, 1999.

[34] N. H. Florin and A. T. Harris, "Hydrogen production from biomass coupled with carbon dioxide capture: The implications of thermodynamic equilibrium," *International Journal of Hydrogen Energy*, vol. 32, no. 17, pp. 4119–4134, 2007.

[35] M. Rydén and A. Lyngfelt, "Using steam reforming to produce hydrogen with carbon dioxide capture by chemical-looping combustion," *International Journal of Hydrogen Energy*, vol. 31, no. 10, pp. 1271–1283, 2006.

[36] M.-B. Andrés, T. Boyd, J. R. Grace, C. J. Lim, A. Gulamhusein, B. Wan, H. Kurokawa, and Y. Shirasaki, "*In-situ* CO_2 capture in a pilot-scale fluidized-bed membrane reformer for ultra-pure hydrogen production," *International Journal of Hydrogen Energy*, vol. 36, no. 6, pp. 4038–4055, 2011.

[37] M. Widyawati, T. L. Church, N. H. Florin, and A. T. Harris, "Hydrogen synthesis from biomass pyrolysis with in situ carbon dioxide capture using calcium oxide," *International Journal of Hydrogen Energy*, vol. 36, no. 8, pp. 4800–4813, 2011.

[38] S. M. Kim, J. D. Lee, H. J. Lee, E. K. Lee, and Y. Kim, "Gas hydrate formation method to capture the carbon dioxide for pre-combustion process in IGCC plant," *International Journal of Hydrogen Energy*, vol. 36, no. 1, pp. 1115–1121, 2011.

[39] C.-C. Cormos, F. Starr, E. Tzimas, and S. Peteves, "Innovative concepts for hydrogen production processes based on coal gasification with CO_2 capture," *International Journal of Hydrogen Energy*, vol. 33, no. 4, pp. 1286–1294, 2008.

[40] M. Wang, C.-G. Lee, and C.-K. Ryu, "CO_2 sorption and desorption efficiency of Ca_2SiO_4," *International Journal of Hydrogen Energy*, vol. 33, no. 21, pp. 6368–6372, 2008.